Geological Survey of Canada
Open File 8548

PROACTIVE INFRASTRUCTURE MONITORING AND EVALUATION (PRIME) INSTALLATION IN CANADA: PROTECTING NATIONAL RAILWAYS BY MONITORING MOISTURE IN AN ACTIVE LANDSLIDE NEAR ASHCROFT, BRITISH COLUMBIA

D.H. Huntley[1], P.T. Bobrowsky[2], R.F. MacLeod[2], R.B. Cocking[1], J.M.R. Joseph[1], K. Sattler[3], D. Elwood[3], J.L. Holmes[4,5], J.E. Chambers[5], P.I. Meldrum[5], P.B. Wilkinson[5], M.T. Hendry[6], and R. Macciotta[6]

INTRODUCTION

In western Canada (**Fig. 1**), the majority of rail freight and passenger trains to the port city of Vancouver (**V**) pass through the landslide-prone Thompson River valley in British Columbia. Landslides studies in this vital transportation corridor began in the late 19th Century. In the early 21st Century geotechnical investigation, remote sensing, and global positioning technologies monitor slope instability.

These methods, combined with terrain mapping and geophysical surveys have provided necessary sub-surface information to understand the spatial and temporal variations in activity at Ripley Landslide (**RL**), 7 km south of Ashcroft (**A**). This is a small feature (approximately 0.4 x 10^6 m^3) but representative of landslides failing in this portion of the transportation corridor. The landslide is of importance since both national railway companies (Canadian National Railways, CN; Canadian Pacific Railways, CPR) have their tracks and infrastructure traversing the landslide (Bunce and Chadwick 2012; **Fig. 2**).

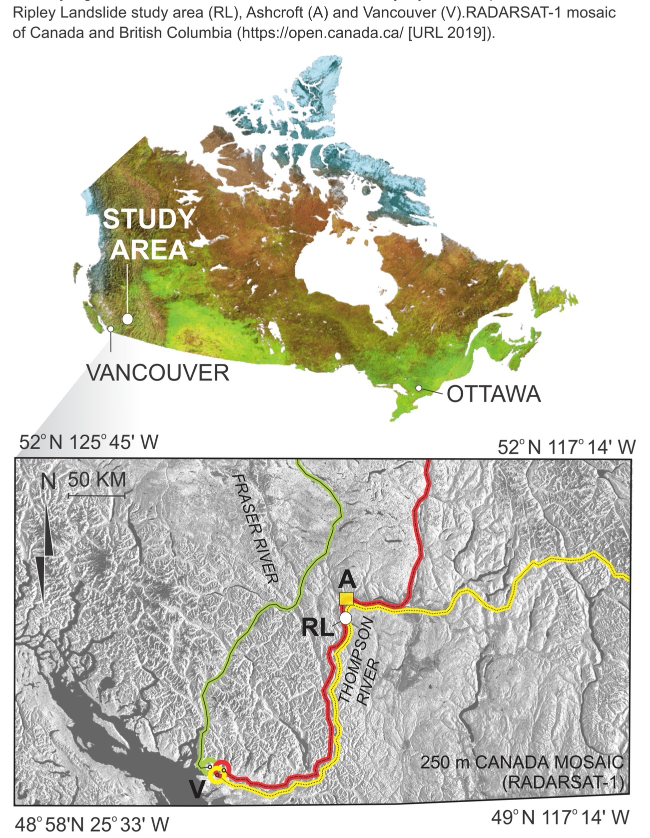

Fig. 1 Rail transportation corridors in southwestern British Columbia (Canadian National Railways, green and red lines; Canadian Pacific Railways, yellow line) with locations of the Ripley Landslide study area (RL), Ashcroft (A) and Vancouver (V).RADARSAT-1 mosaic of Canada and British Columbia (https://open.canada.ca/ [URL 2019]).

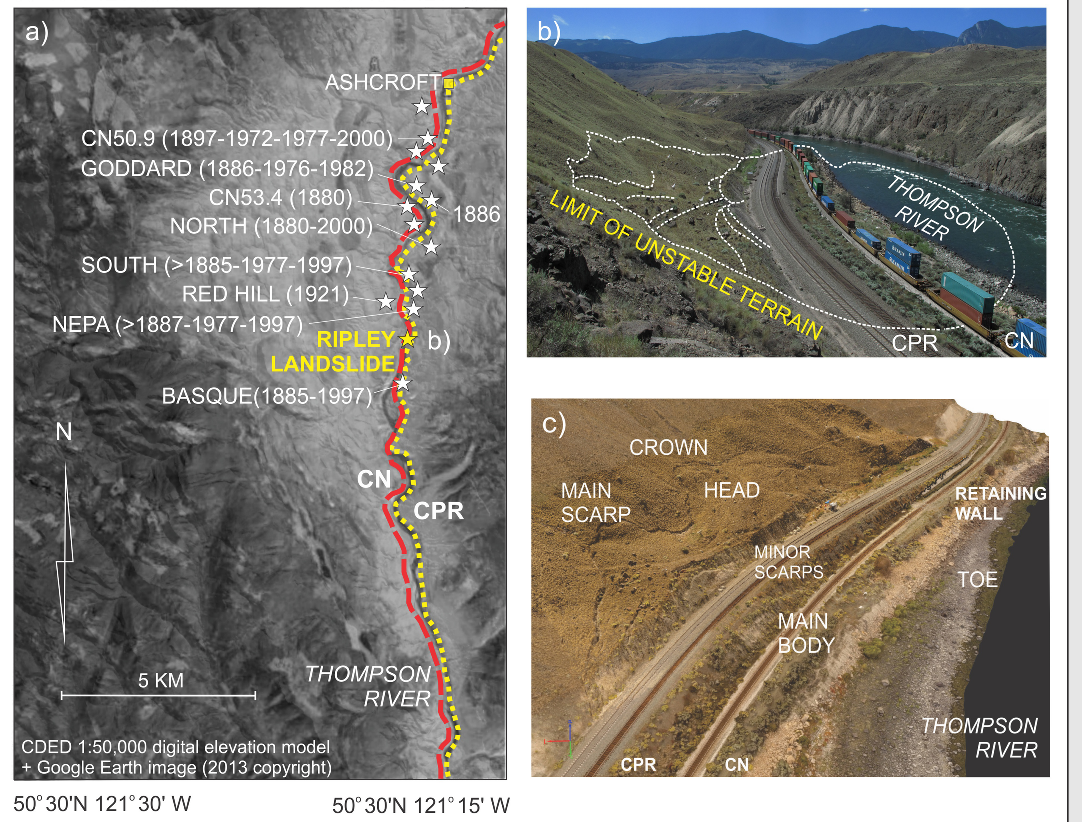

Fig. 2 a) Landslides of the Thompson River valley rail transportation corridor, with location of Ashcroft, Ripley Landslide, and the railway transportation corridor (CN, red dashed line; CPR, yellow dotted line). b) Ripley Landslide showing the approximate extent on land and under Thompson River – view south. c) View southeast showing major surface features on a 2018 structure from motion digital surface model (DSM) (captured and processed by R. MacLeod, GSC).

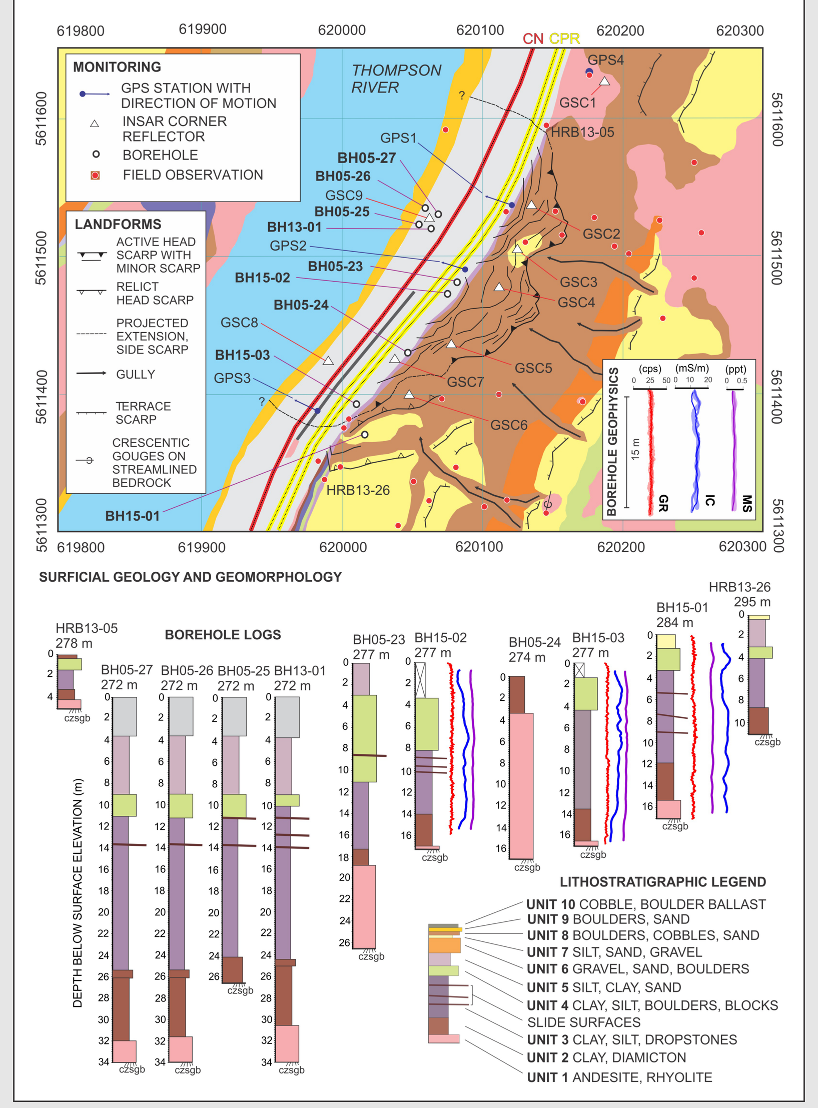

Fig. 3 Surficial hydrogeological units and landforms of Ripley Landslide and adjacent terrain (modified from Huntley and Bobrowsky 2014) with location of GNSS ground position stations (GPS1-4), InSAR corner reflectors (GSC1-9) and boreholes with installed piezometers and inclinometers (BH05-23 to BH05-27, BH13-01, and BH15-01 to BH15-03). Lock-block retaining wall – grey line. Map projection NAD83 Zone 10. Terrain mapping and borehole logs reveal a 30 m-deep bedrock basin infilled with fine-grained sedimentary sequences related to the last glaciation. Slope movement occurs along sub-horizontal shear planes in sub-till clay deposits (brown lines).

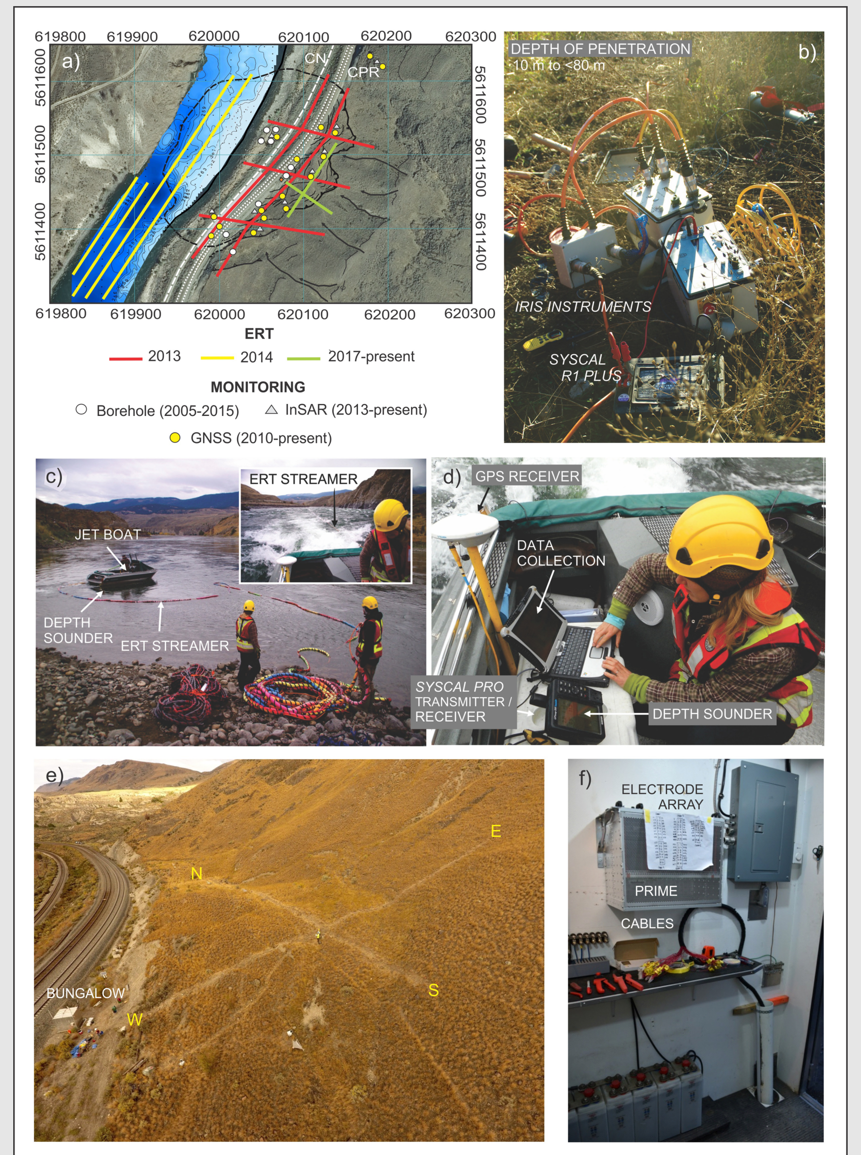

Fig. 4 Geophysics at Ripley Landslide: a) location of terrestrial and waterborne ERT surveys (2013 to 2017) and surface monitoring installations (GNSS and InSAR), map projection NAD83 Zone 10, north to top of map; b) terrestrial ERT set-up; c) and d) waterborne ERT set-up; e) unmanned aerial vehicle (UAV) oblique air photograph looking northeast, showing the north-south (N-S) and east-west (E-W) oriented electrode arrays and CPR bungalow housing the PRIME system developed by the British Geological Survey (captured by R. MacLeod, GSC); f) inside the CPR bungalow showing the PRIME unit with composited cables to be installed according to the position of ground electrodes on the arrays.

GEOPHYSICAL CAMPAIGNS (2013 to 2016)

Terrain mapping, Global Navigation Satellite Systems (GNSS), Interferometric analysis of synthetic radar (InSAR), fibre optic technologies and borehole instrumentation reveal limited information on the subsurface range of earth materials, structures and hydrological function of Ripley Landslide (**Huntley and Bobrowsky 2014**; **Macciotta et al. 2014**; **Hendry et al. 2015**; **Schafer et al. 2015**; **Huntley et al. 2016**; **Huntley et al. 2017a**; **Journault et al. 2018**; **Fig 3**). To address these knowledge gaps, a field program combining conventional geophysical techniques addressed uncertainties by providing new information on the distribution and stratigraphy of terrain deposits, the internal architecture of the landslide, and controls on style of mass wasting at the site (**Huntley et al. 2017b, 2017c**).

Since November 2013, land and water surveys have included electrical resistivity tomography (ERT; **Fig. 4** a-d), frequency electro-magnetic conductivity (FEM), ground penetrating radar (GPR), primary wave refraction (PWR), and multispectral analysis of shear waves (MASW). Downhole geophysical methods employed included natural gamma radiation (GR), induction conductivity (IC) and magnetic susceptibility (MS). The most complete information regarding the internal structure of the landslide was provided by the resistivity surveys. Seismic surveys yielded information at depth, but their detail was less than that provided by the ERT data. Although FEM only imaged the upper 10 m, survey results were consistent with the ERT data and added additional and useful information of the near surface resistivity/conductivity distribution.

MERGING TERRESTRIAL AND WATERBORNE DATASETS

Averaged values of resistivity encompassed within the geometry of the four electrodes used for each measurement were not specific to a particular layer or material so are 'apparent resistivity' measurements. Resistivity data were processed using RES2DINV (**Geotomo Software 2012**) to create 2D resistivity pseudo-sections of the subsurface (**Huntley et al. 2017b, 2017c**).

A forward modelling subroutine was first used to calculate the apparent resistivity values for a given model. Then a non-linear least-squares optimization technique was used by the inversion routine to compare the calculated apparent resistivity values against the measured values. Based on this comparison, the model was then iteratively modified to minimize the difference. The five terrestrial ERT (Wenner-Schlumberger array) and four waterborne ERT datasets (reverse Wenner array) were then merged into a single file and inverted using Loke's RES3DINV inversion program to produce significantly deeper resistivity values than available in 2D profiles (**Geotomo Software 2012**; **Best et al. 2018**).

This 3D inversion resistivity block model was divided into depth slices at 10 m intervals between 200 m and 280 m elevation for the discussion following (**Fig. 5**). Terrestrial and waterborne ERT datasets were also combined and visualized as a pseudo-3D model of resistivity values using ParaView® software. This representation was interpretation-oriented, with the selection of resistivity thresholds at 80 Ωm and 110 Ωm determined by earth materials observed at surface and logged in boreholes (**Fig 3**, **Fig. 5**).

In **Fig. 5**, electrically resistive earth materials (>110 Ωm) are coloured red. They include undersaturated sand and gravel, glacial diamicton (till) and competent bedrock. Saturated bedrock, clay, till and gravel containing soil water are all conductive bodies (<80 Ωm) and coloured blue.

CONTINUOUS ERT DATA ACQUISITION (2017 to Present)

Merged 2D datasets captured a clear, static proxy image of soil moisture and groundwater conditions in surficial deposits and bedrock during November 2013 (land) and 2014 (river). With lithology and porosity as fixed baselines, variations in electrical resistivity over time reflect ground moisture and temperature changes in the landslide (**Bobrowsky et al. 2017**; **Holmes et al. 2018**; **Sattler et al. 2018**).

Between August and November 2017, continuous (real-time) ERT monitoring was deployed to characterize the long-term hydrological behaviour of geological units in the landslide (**cf. Uhlemann et al. 2017**). Two intersecting Wenner arrays were permanently installed in 20 cm-deep trenches dug across the slide body and crown: a north-south array was 91 m-long with 45 evenly spaced ground electrodes; and an east-west array was 54 m-long with 27 electrodes (**Fig. 4** e). Cables and electrodes were wrapped in foam to insulate against the elements and encased within plastic pipe in high-traffic areas, then buried with soil and capped with small boulders to protect against damage by animals (**Fig. 6**).

Composited cables were connected to a ***PR**oactive **I**nfrastructure **M**onitoring and **E**valuation (**PRIME**)* system with continuous 12 V power supply and internet access via a modem (**Fig. 4** f). Apparent resistivity pseudo-sections were processed using RES2DINV (**Geotomo Software 2012**) to create a 2D resistivity model of the sub-surface for December 2017 (**Fig. 6**). This shows a coarse-grained colluvial unit with high apparent resistivity (>500 Ωm) overlying fine-grained glaciolacustrine and morainal units with low to moderate apparent resistivities (<50-200 Ωm). The percentage change in resistivity ground values from this baseline are also presented in **Fig. 6**, with red shading indicating an increase in resistivity (i.e., the ground becoming less conductive), and blue shading indicating a decrease in resistivity (i.e., ground becoming more conductive) between December 2017 and May 2018.

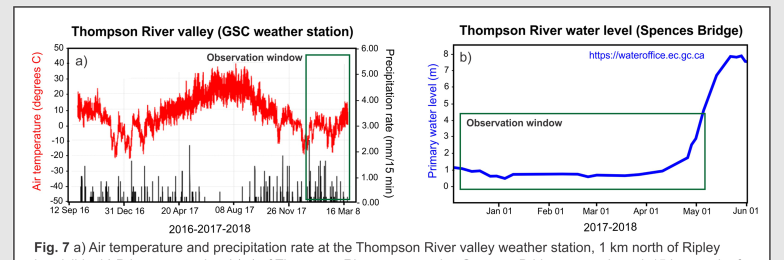

Fig. 7 a) Air temperature and precipitation rate at the Thompson River valley weather station, 1 km north of Ripley Landslide; b) Primary water level (m) of Thompson River, measured at Spences Bridge, approximately15 km south of Ripley Landslide.

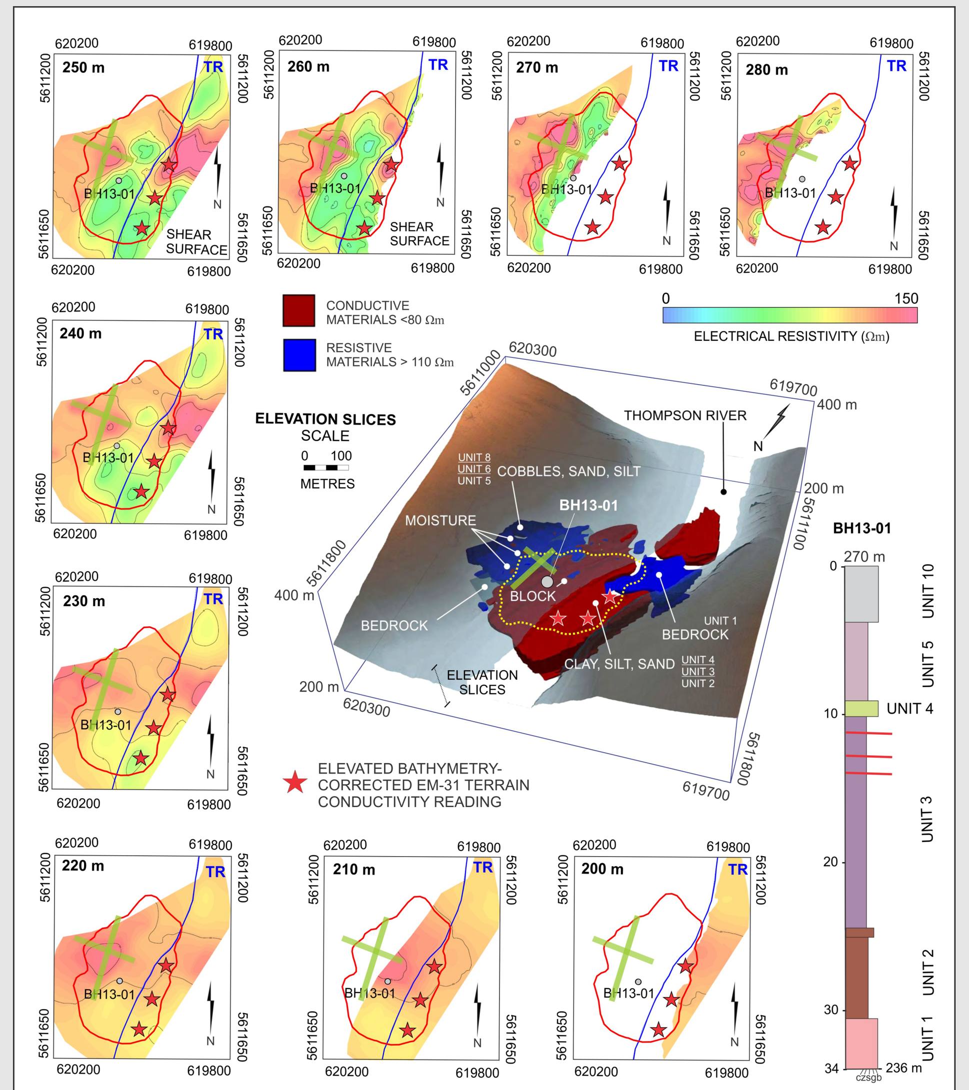

Fig. 5 Merged pseudo-3D ERT depth slices capture a clear static proxy image of ground conditions during autumn. Resistive earth materials include bedrock (unit 1), cobble-rich outwash (unit 6), and hillslope colluvium (unit 8). Conductive earth materials include clay-rich glaciolacustrine beds (units 2, 3 and 5), till diamicton (unit 4), and outwash (unit 6); all of which contain groundwater. Location of BH13-01 shown, graphic log captures changes in hydrogeological units at depth near the centre of the slide body. Blue line represents the east bank of Thompson River (TR). To correspond with the 3D block diagram, north is to bottom of each 2D-depth slice. Map projection NAD83 Zone 10.

BELOW THE RAILWAY TRACKS

On ERT depth slices between 200 m to 220 m elevation (**Fig. 5**), resistivity values vary from 88 Ωm to >120 Ωm, consistent with competent andesite and rhyolite (unit 1) as evidenced by observed outcrops and the recovery of massive bedrock from boreholes (**Fig. 3**). It is possible there is a layer of weathered, less competent regolith overlying the bedrock layer causing the slightly lower resistivity values layered on top (i.e., a coarse basal facies of unit 2). Along the northern and southern landslide boundaries, a transition from bedrock to saturated clay-rich glacial sediments beneath the river is recorded by a drop in resistivity values to below 80 Ωm between 220 m and 240 m elevation (**Fig. 5**).

Lower resistivity values above bedrock are interpreted to represent thin-bedded sand, gravel, clast-supported diamicton, and deformed clay. This sequence is similar to deposits observed in outcrop overlying bedrock exposures (unit 2). From 220 m to 270 m elevation, ERT depth slices show that conductive earth materials (<80 Ωm) are bounded by resistive zones (>140 Ωm) beneath the river and east valley slope (**Fig. 5**). Based on resistivity values, field observations, and borehole information, this area likely comprises glaciolacustrine clay and silt (units 3 and 5), and clay diamicton (till, unit 4). This depositional pattern is interpreted to represent a north-south oriented bedrock palaeochannel fragment infilled with remobilized glacial deposits.

The pseudo-3D model shows a significant portion of the landslide lying below river level (approximately between 230 m and 270 m elevation), with the main slide body represented as an ovate conductive zone (<80 Ωm) containing inliers of resistive material (>120 Ωm) along the northern, eastern, and southern flanks (**Fig. 5**). These latter features are interpreted as locally-derived bedrock blocks that were remobilized during glaciation. Surface and borehole monitoring indicate the landslide moves very slowly (cumulatively <55 mm/yr) on gentle (>2° to <3°) channel-sloping failure planes developed in weak, highly plastic layers of glaciolacustrine silt and clay (**Fig. 3**). The 250 m and 260 m elevation ERT depth slices show that these failing sediments are conductive, saturated with groundwater, and extend under the river (**Fig. 3**).

ABOVE THE RAILWAY TRACKS

Upslope of the river floodplain and railway ballast, at elevations from 270 m to 280 m, ERT depth slices intersect resistivity values in excess of 140 Ωm (**Fig. 5**). This range in values is consistent with unsaturated silt, sand and cobble colluvium overlying bedrock mapped in the field and in boreholes (**Fig. 3**). Relatively lower resistivity values (>50 Ωm and <100 Ωm) suggest the presence of groundwater in fine-grained glaciolacustrine material (units 2, 3 and 5), till diamicton (unit 4), glaciofluvial gravel (unit 6), and alluvial fan deposits (unit 7). The distribution of groundwater in consistent with surface water infiltrating through vertical and horizontal tension fractures into the underlying glaciolacustrine beds and colluvium (units 2 and 3) and bedrock (unit 1).

Scree observed at the steepest point on the easternmost part of the slide body (unit 8) accounts for the higher resistivity values close to the surface (**Fig. 5**). The distribution of these units suggests a 290 m elevation limit to eastward headscarp retrogression and potential maximum volume of approximately 0.8 x 10^6 m^3 for the landslide. Resistive surficial material, starting on the western side of the CN rail tracks and ending in the Thompson River bed, consists of the alluvial boulder field exposed between the coarse rail ballast (unit 10) and low water mark at the river's edge (unit 9). Tension cracks in these unconsolidated materials are surface expressions of active translational or rotational movement along slide planes within the high conductivity layer below. Borehole logs and ERT profiles suggest these failure surfaces are developed in underlying till (unit 4) and glaciolacustrine clay (units 2 and 3).

Above the headscarp, zones of higher conductivity occur where soil water is migrating toward the water table through silt, sand, and cobbles exposed by hill-slope erosion.

PRIME RESULTS AND INTERPRETATION

Rapidly drained coarse-grained colluvial, fluvial, and anthropogenic units have high apparent resistivities (>500 Ωm). Poorly drained fine-grained glaciolacustrine and moraine units have low to moderate apparent resistivities (<50-200 Ωm) (**Fig. 6**).

From 2017 to 2018, changes in ground resistivity are attributed to seasonal variation in sub-surface moisture. Precipitation (rain and snow) and ground temperature (**Fig. 7** a) are recognized as important controls on the distribution of infiltrating soil water and groundwater flux in the slide body. Slope stability at this site is highly sensitive to moisture content.

Between late fall (November) and early spring (February), resistivity values increase in glacial deposits as snowfall blankets the slope, the ground freezes (<0°C) to an estimated depth <2 m, and the river reaches its lowest level (**Fig. 7** b). The greatest displacement rates indicated by GNSS and InSAR occur during winter and spring when transitional ground conditions allow snow melt and rainfall to penetrate deep into the still-frozen (or thawing) slide body by way of tension cracks, planar fractures and bedding surfaces.

From late spring (March) to early fall (October), when ground temperatures are >0°C (i.e., unfrozen), infiltrating precipitation results in a progressive decrease in resistivity at depth as the moisture content of sub-surface clay-rich units increases. Over this period, Thompson River levels are high (**Fig. 7** b) and support the submerged portions of the toe slope. It is during this period that GNSS and InSAR monitoring indicate minimum rates of surface displacement.

EVALUATION OF MULTI-DIMENSIONAL APPROACH

An unprecedented level of insight into the internal composition of the very slow-moving Ripley Landslide has been gained by combining the results of terrestrial, waterborne, and borehole geophysical surveys. These datasets are evaluated in the context of ground observations, surficial geology mapping, and instrumental monitoring (e.g., **Huntley and Bobrowsky 2014; Hendry et al. 2015**; **Journault et al. 2018**).

Small and irregular anomalies, areas of complex subsurface geometry, and groundwater-rich zones are interpreted along all ERT survey lines. Terrain mapping and geophysical surveys indicate a high relief bedrock sub-surface overlain by a 10 m to >30 m-thick package of complex sediments containing groundwater. Planar sub-surface features revealed in surface exposures, borehole logs, and geophysical profiles include tabular bedding and terrain unit contacts (**Fig. 3**, **Fig. 5**). Terrestrial profiles also show discrete curvilinear features interpreted as rotational-translational failure planes in clay-rich beds in the main body of the slide beneath the rail ballast and retaining wall (**Fig. 6**).

Continuous (real-time) ERT monitoring has now been deployed to characterize the long-term hydrological behaviour of geological units in the landslide (**Bobrowsky et al. 2017**; **Holmes et al. 2018**; **Sattler et al. 2018**). This installation is capturing dynamic (4D) changes in electrical resistivity of the hydrogeological units in the landslide. A real-time database is helping to better define surface water and groundwater flow paths in the main slide body, and their relationship to fluctuating pore-water pressures and landslide activity.

In turn, this monitoring will improve our understanding of soil strength and landslide stability. Understanding the impact of season variations in ground resistivity will enable us to develop moisture paths and thresholds for the prediction of slope failure at Ripley Landslide and, by extension, other slides in the Thompson River transportation corridor.

ACKNOWLEDGEMENTS

Research presented in this publication was undertaken as part of the International Consortium on Landslides (ICL) International Programme on Landslides (IPL) Project 202. Activities at this site have led to World Centre of Excellence on landslide disaster reduction recognition for both the Geological Survey of Canada and the University of Alberta (iplhq.org). Research was funded by Transport Canada and Natural Resources Canada. For their geophysical services, we wish to thank Neil Parry, Megan Caston, Cassandra Budd and Gordon Brasnett (EBA-TetraTech, Edmonton, Alberta) in 2013-2014; Paul Bauman, Landon Woods and Kimberly Hume (Advisian, Worley Parsons Group, Calgary, Alberta) in 2014-2015; Cliff Candy, Larry Theriault, Caitlin Gugins and Heather Ainsworth (Frontier Geosciences Inc., North Vancouver, BC) in 2015-2017; and Mel Best (BEMEX Consulting International) from 2014-2019. Fieldwork would not be possible without the support of Trevor Evans (Canadian National Railway, Kamloops, BC) and Danny Wong (Canadian Pacific Railway, Calgary, Alberta). This open file poster was presented at the 32nd Annual Meeting of the Environmental and Engineering Geophysical Society in Portland, Oregon, USA in March 2019. Open File 8548 was edited by Carol Wagner (GSC-Pacific) and critically reviewed by Nathan Hayward (GSC-Pacific).

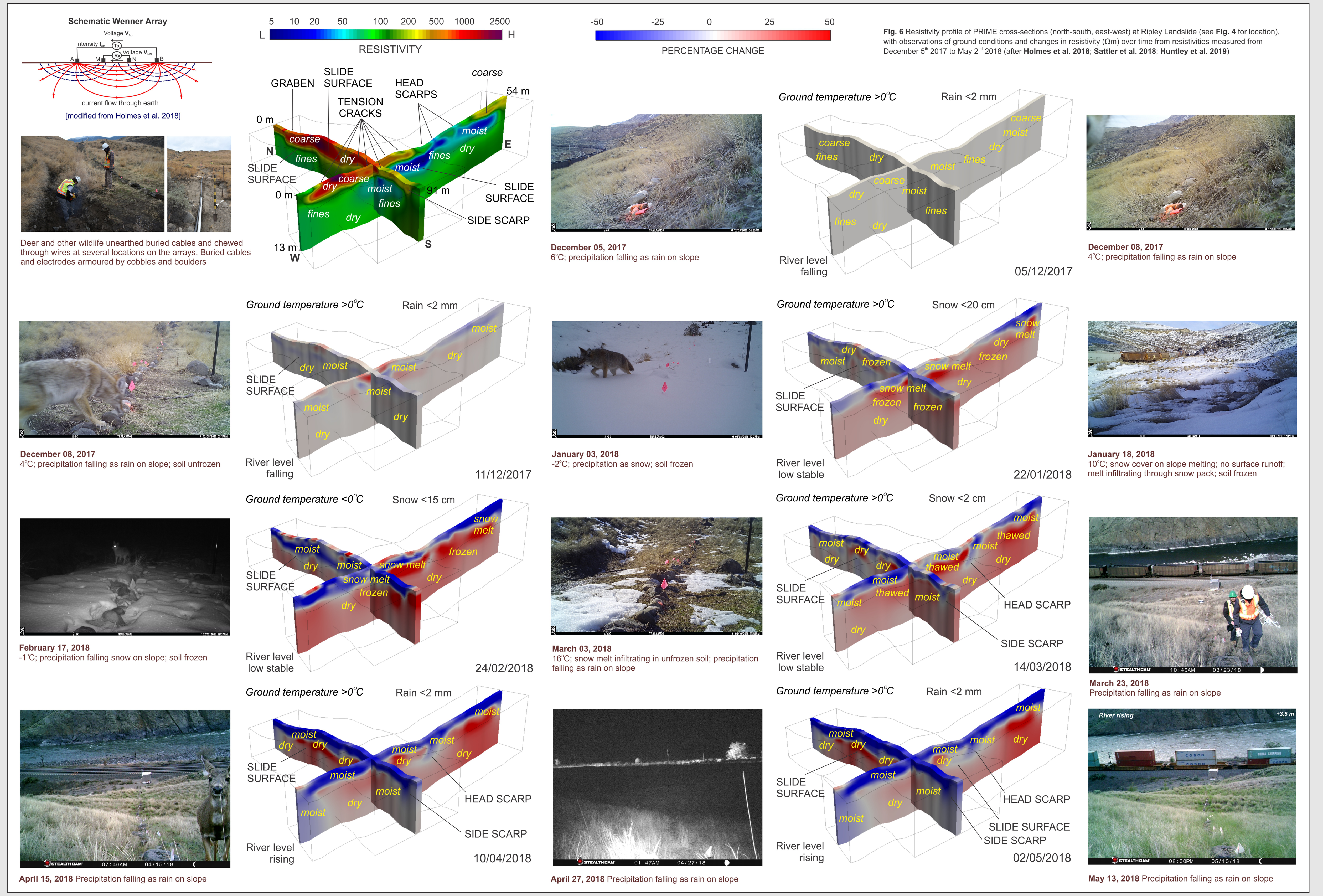

Fig. 6 Resistivity profile of PRIME cross-sections (north-south, east-west) at Ripley Landslide (see **Fig. 4** for location), with observations of ground conditions and changes in resistivity (Ωm) over time from resistivities measured from December 5th 2017 to May 2nd 2018 (after **Holmes et al. 2018**; **Sattler et al. 2018**; **Huntley et al. 2019**).

REFERENCES

Best M, Bobrowsky P, Huntley D, Macciotta R, Hendry M (2018) Integrating terrestrial and waterborne ERT surveys at the Ripley Landslide, near Ashcroft, British Columbia. In: Proceedings Volume 31st SAGEEP Annual Meeting, Environmental and Engineering Geophysical Society, Nashville, Tennessee, USA, 1 p

Bobrowsky P, Huntley D, Neelands P, MacLeod R, Mariampillai D, Hendry M, Macciotta R, Reeves H, Chambers J (2017) Ripley Landslide – Canada's premier landslide field laboratory. In: Proceedings Volume of the Geological Society of America Annual Meeting, Seattle, Washington, USA, 1 p

Bunce C, Chadwick I (2012) GPS monitoring of a landslide for railways. In: Eberhardt et al. (eds.), Landslides and Engineered Slopes: Protecting Society through Improved Understanding, pp 1373-1379

Hendry M, Macciotta R, Martin D (2015) Effect of Thompson River elevation on velocity and instability of Ripley Slide. Canadian Geotechnical Journal 52(3): 257-267

Holmes J, Chambers J, Donohue S, Huntley D, Bobrowsky P, Meldrum P, Uhlemann S, Wilkinson P, Swift R (2018) The Use of Near Surface Geophysical Methods for Assessing the Condition of Transport Infrastructure. Civil Engineering Research Association, Special Issue on Structural Integrity of Civil Engineering Infrastructure, Journal of Structural Integrity and Maintenance, 6 p

Huntley D, Bobrowsky P (2014) Surficial geology and monitoring of the Ripley Slide, near Ashcroft, British Columbia, Canada. Geological Survey of Canada Open File 7531, 21 p

Huntley D, Bobrowsky P, Zhang Q, Zhang X, Lv Z, Hendry M, Macciotta R, Schafer M, Le Meil G, Journault J, Tappenden K (2016) Application of Optical Fibre Sensing Real-Time Monitoring Technology at the Ripley Landslide, near Ashcroft, British Columbia, Canada. In: Proceedings Volume of Canadian Geotechnical Society Annual Meeting, GeoVancouver 2016, 13 p

Huntley D, Bobrowsky P, Charbonneau F, Journault J, Hendry M (2017a) Innovative landslide change detection monitoring: application of space-borne InSAR techniques in the Thompson River valley, British Columbia, Canada. In: Landslide Research and Risk Reduction for Advancing Culture and Living with Natural Hazards - Volume 3, 4th World Landslide Forum (ICL-IPL), Ljubljana, Slovenia, Springer Nature, 13 p

Huntley D, Bobrowsky P, Parry N, Bauman P, Candy C, Best M (2017b) Ripley Landslide: the geophysical structure of a slow-moving landslide near Ashcroft, British Columbia, Canada. Geological Survey of Canada Open File 8062, 59 p

Huntley D, Bobrowsky P, Best M (2017c) Combining terrestrial and waterborne geophysical surveys to investigate the internal composition and structure of a very slow-moving landslide near Ashcroft, British Columbia, Canada. In: Landslide Research and Risk Reduction for Advancing Culture and Living with Natural Hazards - Volume 2, 4th World Landslide Forum (ICL-IPL), Ljubljana, Slovenia, Springer Nature, 15 p

Journault J, Macciotta R, Hendry M, Charbonneau F, Huntley D, Bobrowsky P (2018) Measuring displacements of the Thompson River valley landslides, south of Ashcroft, B.C., Canada, using satellite InSAR. Landslides, 15 (4): 621-636

Macciotta R, Hendry M, Martin D, Elwood D, Lan H, Huntley D, Bobrowsky P, Sladen W, Bunce C, Choi E, Edwards T (2014) Monitoring of the Ripley Slide in the Thompson River Valley, B.C. In: Proceedings and Abstracts Volume Geohazards 6 Symposium, Kingston, Ontario, Canada, 1 p

RES2DINV (2012) Rapid 2-D Resistivity & IP inversion using the least-squares method, Geoelectrical Imaging 2D & 3D Geotomo Software, Penang, Malaysia, www.geotomosoft.com

Sattler K, Elwood D, Hendry M, Macciotta R, Huntley D, Bobrowsky P, Meldrum P (2018) Real-time monitoring of soil water content and suction in slow-moving landslide. GeoEdmonton 2018, Proceedings Paper, 8 p

Schafer M, Macciotta R. Hendry M, Martin D, Bobrowsky P, Huntley D, Bunce C, Edwards T (2015) Instrumenting and Monitoring a Slow Moving Landslide. GeoQuebec 2015 – Challenges from North to South, Paper 7 p

Uhlemann S, Chambers J, Wilkinson P, Maurer H, Merritt A, Meldrum P, Kuras O, Gunn D, Smith A, Dijkstra T (2017) Four-dimensional imaging of moisture dynamics during landslide reactivation. Journal of Geophysical Research, 122: 398-418

Natural Resources Canada / Ressources naturelles Canada

[1]Geological Survey of Canada, 1500-605 Robson Street, Vancouver, British Columbia, Canada V6B 5J3
[2]Geological Survey of Canada, 9860 West Saanich Road, Sidney, British Columbia, Canada V8L 4B2
[3]University of Saskatchewan, 57 Campus Drive, Saskatoon, Saskatchewan, Canada S7N 5A9
[4]Queen's University Belfast, University Road, Belfast, United Kingdom BT7 1NN
[5]British Geological Survey, Environmental Science Centre, Keyworth, United Kingdom NG12 5GG
[6]University of Alberta, 9211-116 Street NW, Edmonton, Alberta, Canada T6G 1H9

For more information, please contact D.H. Huntley (david.huntley@canada.ca)

Permanent link: https://doi.org/10.4095/314548

This publication is available for free download through GEOSCAN (http://geoscan.nrcan.gc.ca/)

Recommended citation
Huntley, D.H., Bobrowsky, P.T., MacLeod, R.F., Cocking, R.B., Joseph, J.M.R., Elwood, D., Sattler, K., Holmes, J.L., Chambers, J.E., Meldrum, P.I., Wilkinson, P.B., Hendry, M.T., and Macciotta, R., 2019. Proactive infrastructure monitoring and evaluation (PRIME) installation in Canada: protecting national railways by monitoring moisture in an active landslide near Ashcroft, British Columbia; Geological Survey of Canada, Open File 8548, 1 poster. https://doi.org/10.4095/314548

Canada